Reversible Photoswitchable Inhibitors Enable Wavelength-Selective Regulation of Out-of-Equilibrium Bi-enzymatic Systems

Michael Teders, Nicholas R. Murray, and Wilhelm T. S. Huck*[a]

The construction of synthetic enzymatic reaction networks can provide new insights into the design principles of living systems. However, the programmable connection of enzymes into a wide range of network topologies has been challenging due to the lack of a general strategy enabling a reversible activity regulation of individual network enzymes. Here, we exploit a general and modular strategy based on the external regulation of enzymes using light and photoswitchable inhibitors (PIs) that enables the bottom-up construction and control of enzymatic systems studied under out-of-equilibrium conditions. Upon synthesis and incorporation of potent photoswitchable trypsin inhibitors (Tr-PIs), the output of several functional enzymatic systems could be photoregulated using 390/460 nm light as a trigger signal. In addition, the wavelength-selective control over the activity of two enzymes within a functional bi-enzymatic system was achieved using a suitable combination of two PIs.

1. Introduction

In living systems, biochemical processes are organized into complex networks, which are continuously sensing and adapting to changes in the environment.[1] The properties of these networks underlie many of the characteristic capabilities of living systems, such as self-healing, homeostasis, or conversion of chemical energy into directed motion, growth and division.[2–6]

A central goal of systems chemistry is to investigate and translate the common design principles of the enzymatic reaction networks found in nature into a practical and modular approach, thereby ultimately enabling the programmable and rational design of life-inspired systems exhibiting tunable properties.[7–14] In living systems, enzymes are the molecular machines of choice as their activity can be controlled via, for example, post-translational modifications, allosteric interactions, or substrate competition.[2,15–18] In addition, their non-linearity (resulting in sensitive feedback loops), chemical specificity and high turnover numbers make them ideal for converting a wide range of signals into a molecular output. However, the bottom-up construction of (complex) life-inspired systems is particularly challenging due to the lack of a general strategy enabling the reversible and precise regulation of individual network components (e.g., enzymes) and isolated network motifs.

A plethora of different strategies to reversibly and spatiotemporally control the activity of enzymes have been developed in the past decades.[19–26] In a systems chemistry setting, light is an ideal external trigger to regulate enzyme activity,[27,28] and we recently reported that the incorporation of reversible photoswitchable α-chymotrypsin inhibitors (Cr-PIs) generates a non-linear ultrasensitive input-output response when studying enzymatic reactions under out-of-equilibrium conditions.[29] Here, we expand upon our strategy by synthesizing photoswitchable trypsin inhibitors (Tr-PIs) and combining these in the bottom-up construction of photoresponsive modules containing two enzymes (Figure 1). To demonstrate the feasibility of our strategy to control multiple enzymes individually using different wavelengths, we incorporated both a Cr- and a Tr-PI in a bi-enzymatic system.

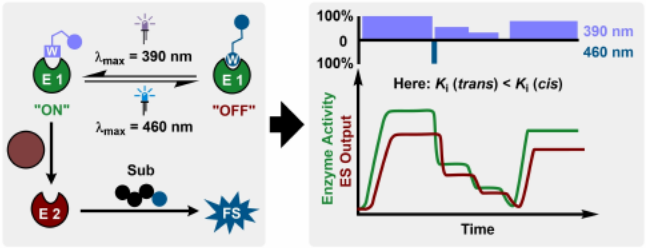

Figure 1. Reversible photocontrol over the output of bi-enzymatic systems by the incorporation of photoswitchable enzyme inhibitors. E = enzyme, Sub = substrate, FS = fluorogenic substrate, ES = functional enzymatic system.

[a] *Dr. M. Teders, N. R. Murray, Prof. W. T. S. Huck*
Institute for Molecules and Materials
Radboud University Nijmegen
Heyendaalseweg 135, 6525 AJ Nijmegen (The Netherlands)
E-mail: w.huck@science.ru.nl

Supporting information for this article is available on the WWW under https://doi.org/10.1002/syst.202100020

2. Results and Discussion

The synthesis of Tr-PIs was performed by applying a chromophore/warhead strategy,[23] aiming to maximize the difference in inhibition constants (K_i) between both isomeric states (switching factor, $SF = K_{i,cis}/K_{i,trans}$), while keeping the other (photo-)physical requirements for later flow applications in mind (e.g., water-solubility, photostability, or photoreversibility). The amidine functionality was identified as a promising warhead due to its competitive mode of inhibition and strong non-covalent interactions with the receptor of trypsin (Tr).[30–32] Because of their excellent photophysical properties and the ease of synthesis,[33] azobenzenes were selected as the chromophore.[23] The optimum inhibitor identified in our study was **Tr-PI** bearing two methoxy substituents in the *ortho* and *para* position of the adjacent arene of the azobenzene unit (Figure 2, see 2.1–4.8 of Supporting Information for synthesis and characterization of all synthesized Tr-PIs). **Tr-PI** exhibits a good solubility in a 99:1 mixture of a commonly used aqueous protease buffer (TRIS (200 mM), Ca^{2+} (20 mM), pH = 7.81) and DMSO. The photophysical characterization of **Tr-PI** revealed both a high photostability and photoreversibility upon 390/460 nm excitation and a slow thermal *cis* to *trans* relaxation ($t_{1/2}$ = 2.55 h), thereby enabling full photocontrol over the isomeric state of **Tr-PI** using light. Importantly, the content of *cis* isomer obtained upon 390 nm irradiation of **Tr-PI** in the buffer was high (PSS = 93 %, see 3.1–3.5 of Supporting Information for details regarding photophysical characterization of **Tr-PI**). Using **Tr-PI**, the protease trypsin, *N*-benzoyl-Arg-7-amido-4-methylcoumarin (R-AMC) as substrate and TRIS/Ca^{2+}/BSA (200 mM, 20 mM, 0.1 w-%, pH = 7.81) with 1.0 vol-% DMSO as buffer, we determined the inhibition constants for the enzyme-inhibitor interaction of *trans*/*cis*-**Tr-PI** and Tr using a fluorogenic AMC-based assay.[34] The photoswitchable trypsin inhibitor is a strong competitive inhibitor in its *trans* state ($K_{i,trans}$ = 4.3 ± 0.1 μM) and turns into a weaker inhibitor upon 390 nm photoinduced *trans-cis* isomerization ($K_{i,cis}$ = 33.0 ± 1.7 μM). Although less pronounced compared to our previously reported highly potent photoswitchable α-chymotrypsin inhibitor,[29] the resulting switching factor of 7.7 still offers a sufficient level of photocontrol over the activity of Tr. In batch experiments, we achieved reproducible reversible photoswitching cycles indicating a competitive mode of inhibition and sufficient stability of trypsin with regard to prolonged 390/460 nm light irradiation (see 4.5 of Supporting Information for details).

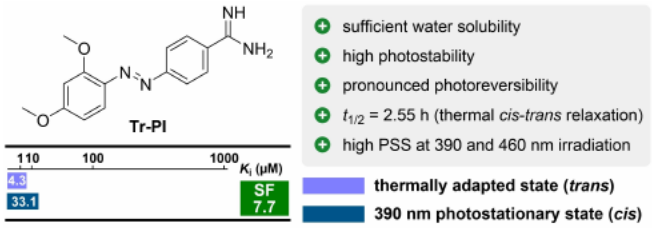

Figure 2. Structure and enzymological data of the photoswitchable trypsin inhibitor **Tr-PI** identified throughout structure-activity-relationship analysis. Inhibition constants were determined using a fluorogenic assay. For details on other synthesized photoswitchable trypsin inhibitors, experimental procedures and results, see 2.1–4.8 of Supporting Information. SF = switching factor; PSS = photostationary state.

We next sought to apply our synthesized **Tr-PI** for the bottom-up construction and photoregulation of enzymatic systems studied under out-of-equilibrium conditions. We therefore constructed a highly automated and programmable microfluidic flow setup featuring a continuously-stirred tank reactor (CSTR) as the central element (Figure 3A). All irradiation parameters, for example, its timing, the duration, the photon flux or the choice of the irradiation source, can be reproducibly controlled (see 8.1 and 9 of Supporting Information for details on the flow setup and information on the computer code to reproducibly control the irradiation parameters).

The AMC production of an enzymatic system based on the autocatalytic activation of trypsinogen by trypsin could be reversibly photoregulated under out-of-equilibrium conditions by incorporation of **Tr-PI** (Figure 3B). Upon irradiation with 390 nm light, the thermally adapted *trans*-**Tr-PI** is converted into the weaker inhibitory *cis* isomer, which results in an increased Tr activity and higher levels of observed AMC production (see 8.2.2 of Supporting Information). Importantly, by varying the light intensity, the effective inhibitor strength can be gradually altered, thereby enabling fine-tuning of the kinetics of enzyme-catalyzed reactions using light as external stimuli.[35] By installing 390 and 460 nm light pulses with different intensities and durations, the output of the enzymatic system can be precisely and reproducibly regulated (see 8.2.2 of Supporting Information for experimental results and details). In the absence of a 460 nm light pulse for photoinduced *cis* to *trans* isomerization of **Tr-PI**, an exponential decay in AMC concentration with time was observed (Figure 3B, green curve).

The weaker inhibitory *cis* isomer is flushed out of the reactor over time. The thermal *cis* to *trans* relaxation is slow for **Tr-PI** due to the long half-life of this species ($t_{1/2}$ = 2.55 h). In contrast, a faster decrease in AMC concentration can be observed after irradiation of the CSTR with 460 nm light (Figure 3B, blue curve). In this case, photoinduced *cis* to *trans* isomerization occurs, resulting in quicker recovery to the AMC values prior to UV irradiation.

In addition, we photocontrolled the trypsin-catalyzed formation of α-chymotrypsin from its inactivated zymogen chymotrypsinogen (Cg) via the incorporation of **Tr-PI** (Figure 3C).[36] By using N-succinyl-Ala-Ala-Pro-Phe-7-amido-4-methylcoumarin (Suc-AAPF-AMC) as substrate, we detect the activation of the cascade as AMC can only be produced upon cleavage by Cr. As depicted in Figure 3D, increasing the photon flux of 390 nm irradiation leads to a higher AMC output of the enzymatic system due to the formation of the weaker Tr-inhibiting *cis* isomer of **Tr-PI**. However, as Cr is part of a cascade, the increase in AMC output is delayed with respect to increasing the 390 nm photon flux. Low light intensities do not cause a significant rise of the AMC steady state concentration and are being filtered, as **Tr-PI** is not substantially isomerized to the weaker inhibitory *cis* isomer (low PSS). Upon gradually increasing the photon flux, an almost linear increase in AMC steady state concentration was

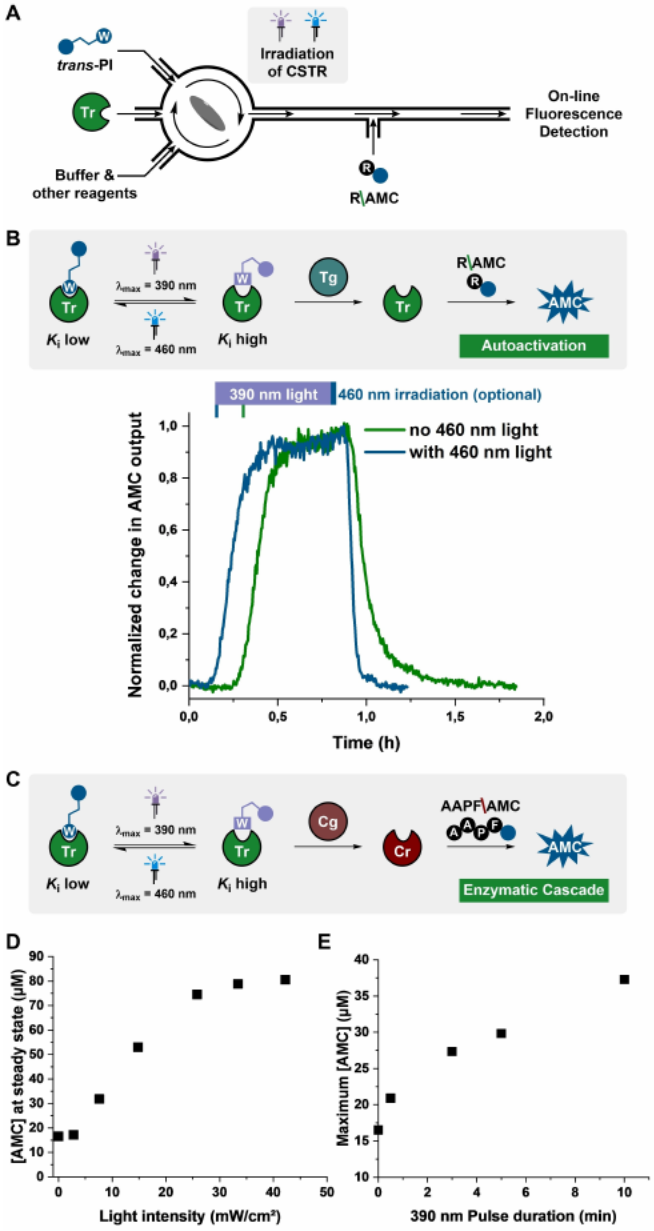

Figure 3. A) Schematic of experimental flow setup applied for the performance of out-of-equilibrium experiments. **B)** Reversible photoregulation of a Tr/Tg-based autoactivation enzymatic system. The Tr activity is controlled using light via the incorporation of **Tr-PI**. Concentrations in flow cuvette: [Tr] = 33 nM, [**Tr-PI**] = 83.3 μM, [R-AMC] = 166.6 μM, [Tg] = 1.66 μM. Flow rates: Tr, **Tr-PI**, Tg = 200 μL/h; R-AMC = 400 μL/h, buffer = 200 μL/h. Reactor volume = 196 μL. For details on experimental procedure and light pulse sequences, see 8.2.2 of Supporting Information. **C)** Network motif of the enzymatic cascade based on the Tr-catalyzed generation of α-chymotrypsin from chymotrypsinogen. The Tr activity is controlled using light via the incorporation of **Tr-PI. D**) Impact of 390 nm light intensity variation on the steady state AMC output concentration. **E**) Impact of 390 nm pulse duration on the maximum AMC concentration observed after irradiation. Concentrations in flow cuvette in **D**) and **E**): [Tr] = 40 nM, [**Tr-PI**] = 75 μM, [AAPF-AMC] = 192 μM, [Cg] = 0.5 μM. Flow rates: Tr, **Tr-PI**, AAPF-AMC = 200 μL/h; Cg = 50 μL/h, buffer = 350 μL/h. Reactor volume = 196 μL. For details on experimental procedure and light pulse sequences, see 8.2.3 of Supporting Information.

observed, before the maximum AMC output of the system was reached at roughly 35 mW/cm^2. Irradiation with 390 nm LED pulses at 100% intensity causes the formation of AMC peaks, which increase in amplitude along with increased pulse durations (Figure 3E). Even short UV pulses cause the formation of AMC peaks, as the weaker-inhibitory *cis* isomer of **Tr-PI** is only removed due to efflux from the reactor over time.

In order to control more complex functional systems, which are often the result of numerous interconnected processes,[4] multiple molecular operations would have to be controlled independently. Using light as stimulus, this can be achieved by incorporating various photoactive molecular effectors with different photophysical properties. Surprisingly, to date, only a few realizations of reversible, wavelength-selective photoswitching have been reported.[37–40] In our recent work, we developed a highly potent competitive inhibitor of the serine protease α-chymotrypsin (Cr), featuring a trifluoroborate functionality as warhead (**Cr-PI**, see Figure 4A).[29] By comparing the

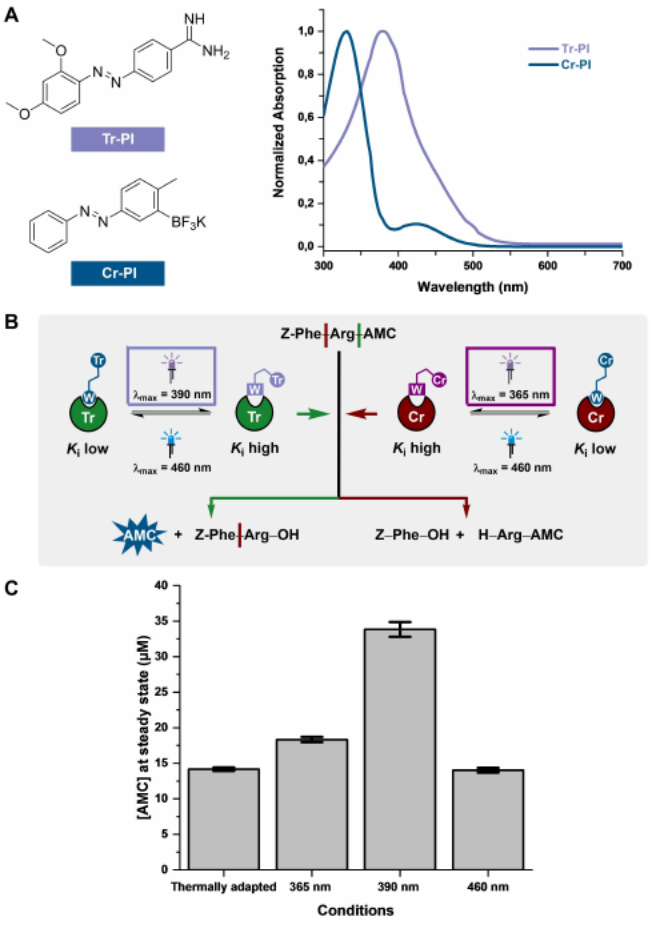

Figure 4. A) UV/vis absorption spectra of **Tr-PI** and **Cr-PI. B)** Orthogonal cleavage of FR-AMC by Tr and Cr, photocontrolled via the incorporation of **Tr-PI** and **Cr-PI. C)** Wavelength-selective control over the enzymatic system outlined in **B)**, studied under out-of-equilibrium conditions using **Cr-PI** and **Tr-PI**. Concentrations in flow cuvette: [Cr] = 14 nM, [**Cr-PI**] = 45 μM, [FR-AMC] = 205 μM, [Tr] = 28 nM, [**Tr-PI**] = 34 μM. Flow rates: Cr, FR-AMC, Tr = 600 μL/h; **Cr-PI**, **Tr-PI** = 200 μL/h. Reactor volume = 196 μL. For details on experimental procedures and light pulse sequences, see 8.2.4 of Supporting Information.

UV/vis absorption spectra of **Cr-PI** and **Tr-PI**, we identified significant differences in the wavelength of their π-π* absorption band maxima (Figure 4A). For **Cr-PI**, this maximum is at 330 nm, whereas the maximum of **Tr-PI** is bathochromically shifted to 390 nm due to the installation of two electron-donating methoxy substituents.[41] While the molar extinction coefficients for both compounds only differ by a factor of ~2 at 365 nm ($\varepsilon_{365\,nm}$(**Cr-PI**) = 24032 $M^{-1}cm^{-1}$, $\varepsilon_{365\,nm}$(**Tr-PI**) = 11805 $M^{-1}cm^{-1}$,), a ~9-fold difference in absorption was observed at 390 nm ($\varepsilon_{390\,nm}$(**Cr-PI**) = 2823 $M^{-1}cm^{-1}$, $\varepsilon_{390\,nm}$(**Tr-PI**) = 25804 $M^{-1}cm^{-1}$). Owing to the difference in absorption properties at 390 nm, the *cis* content of both inhibitors at the 390 nm PSS is significantly higher for **Tr-PI** ($PSS_{390\,nm}$ = 96 %) than for **Cr-PI** ($PSS_{390\,nm}$ = 18 %). Thus, the relative activity of Tr can be more strongly increased by 390 nm irradiation ($SF_{390\,nm}$ = 7.7 ± 0.2) than Cr ($SF_{390\,nm}$ = 2.2 ± 0.1). The n-π* absorption band maxima of **Tr-PI** and **Cr-PI** are at wavelengths higher than 420 nm, so that the *cis* to *trans* photoisomerization for both compounds can be induced simultaneously upon 460 nm irradiation. In our enzymatic system, the serine proteases Cr and Tr compete for the cleavage sites of a peptide substrate, Z-Phe-Arg-AMC (FR-AMC, Figure 4B).[36] Cr cleaves the phenylalanine/arginine peptide bond of the substrate, thereby producing Z-Phe-OH and H-Arg-AMC. Tr cleavage leads to the formation of Z-Phe-Arg-OH and AMC. Importantly, while Cr is still able to cleave the phenylalanine/arginine peptide bond of the latter Tr cleavage product, H-Arg-AMC cannot be processed by Tr due to the free N-terminus of the substrate.[36] Thus, AMC can only be obtained upon Tr-catalyzed cleavage of FR-AMC.

By the incorporation of **Tr-PI** and **Cr-PI**, which are both very weak inhibitors of the respective other enzyme (see 4.8 and 7.2 of Supporting Information), the activity of Tr and Cr can be regulated depending on the wavelength of the irradiation source. As shown in Figure 4C, there is a low AMC output in the absence of light ($[AMC]_{steady\text{-}state}$ = 14.2 μM). Both PIs are in their thermally adapted state and thus strong inhibitors of the respective enzymes. Upon irradiating the CSTR with 390 nm light, an increased AMC production was detected ($[AMC]_{steady\text{-}state}$ = 33.8 μM). As previously outlined, the amount of the weaker-inhibitory *cis* isomer of **Tr-PI** formed at 390 nm irradiation is 5.3 times higher than the one of **Cr-PI**. Thus, the activity of Tr is most strongly up-regulated, favoring the arginine/AMC peptide cleavage and increased concentrations of the fluorescent AMC. Irradiation with 365 nm light shifts the PSS of **Cr-PI** to higher concentrations of the weaker-inhibitory *cis* isomer ($PSS_{365\,nm}$ = 93 %), while simultaneously the concentration of *cis*-**Tr-PI** is decreased due to a lower PSS at this wavelength ($PSS_{365\,nm}$ = 62 %). While the activity of Cr is thereby up-regulated ($SF_{365\,nm}$ = 21 ± 4.0), the Tr activity is decreased due to the presence of higher concentrations of the stronger-inhibiting *trans*-**Tr-PI** ($SF_{365\,nm}$ = 3.2 ± 0.1). As a result, there is an increased cleavage of the phenylalanine/arginine peptide bond, leading to a lower AMC production of the enzymatic system bk;($[AMC]_{steady\text{-}state}$ = 18.3 μM). Upon blue light irradiation (460 nm), both PIs are fully converted to their stronger-inhibitory *trans* isomers, so that the AMC output prior to irradiation is recovered ($[AMC]_{steady\text{-}state}$ = 14.1 μM).

To probe the robustness of this bi-enzymatic system with respect to interfering stimuli, we continuously irradiated the CSTR with either 365 nm or 390 nm light while pulsing with the other light source and gradually increasing the pulse duration from 2 sec to 60 min (Figure 5; see 4.8 and 7.4 for kinetic characterization of the photoswitchable inhibitors under 365 and 390 nm irradiation).

Under continuous irradiation with 390 nm and pulsing with 365 nm light, a sigmoidal response curve was obtained where the normalized change in AMC output increases along with increased 365 nm pulse durations (Hill coefficient n = 1.38).[42] Pulses of 5 s already led to a significant change in AMC output, indicating that in this state, the system is quite sensitive to interfering 365 nm pulses. In contrast, constant irradiation with 365 nm and pulsing with 390 nm light, yielded a stronger pronounced sigmoidal response curve (Hill coefficient n = 1.86). Pulses as long as 30 s were filtered out. Thus, the enzymatic system is more sensitive to interfering 365 nm pulses than to 390 nm pulses.

3. Conclusion

We have successfully exploited a general and modular strategy to control functional enzymatic systems under out-of-equilibrium conditions via the incorporation of competitive photoswitchable trypsin and α-chymotrypsin inhibitors. The output of

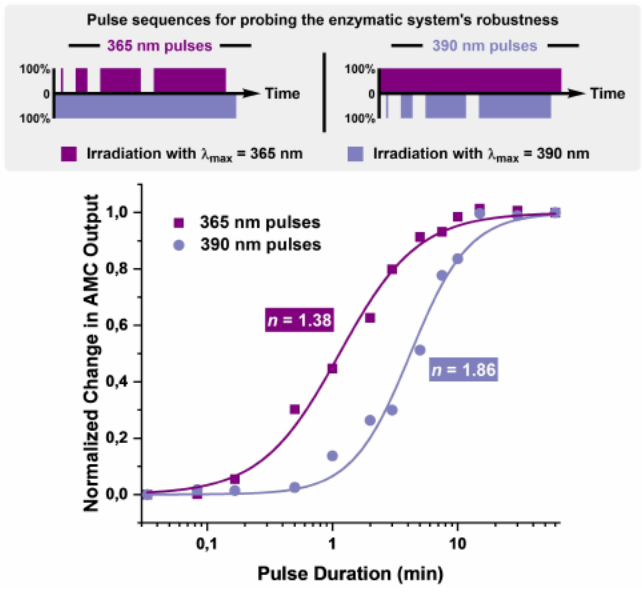

Figure 5. Probing the robustness of the bi-enzymatic system by pulsing with either 365 or 390 nm light while continuously irradiating with the respective other light source. Experimental data has been fitted to the Hill equation (line) to determine the Hill coefficient n as a measure for the enzymatic system's robustness. [Cr] = 14 nM, [**Cr-PI**] = 45 μM, [FR-AMC] = 205 μM, [Tr] = 28 nM, [**Tr-PI**] = 34 μM. Flow rates: Cr, FR-AMC, Tr = 600 μL/h; **Cr-PI**, **Tr-PI** = 200 μL/h. Reactor volume = 224 μL. For details on experimental procedure and light pulse sequences, see 8.2.5 of Supporting Information.

several bottom-up constructed bi-enzymatic systems could be photoregulated using 390/460 nm light as a trigger signal.

To demonstrate the feasibility of our strategy to control multiple enzymes individually using different wavelengths, we incorporated both a Cr- and a Tr-photoinhibitor in a bi-enzymatic system. The wavelength-selective modulation of the bi-enzymatic systems response clearly demonstrates the opportunity to control multiple enzymatic processes within a network using different irradiation sources and thus lays the foundation for further investigations. A combination of our strategy with the immobilization of enzymes, thereby mimicking cellular compartmentalization, is currently being undertaken in our laboratories. By the immobilization of the enzyme "hardware", we can construct complex photocontrolled out-of-equilibrium systems, where the small molecule "software", for example, PIs and substrates, can freely diffuse and interconnect different network modules.

The universal application of reversible photoswitchable inhibitors could allow for the selective and spatiotemporal control of multiple enzymes independently from each other using light – especially within highly complex networks.

Acknowledgements

This project has received funding from the European Union's Horizon 2020 research and innovation programme under grant agreement No 862081 (CLASSY) and the Dutch Ministry of Education, Culture and Science (Gravity program 024.001.035). Generous financial support by the German National Academy of Sciences Leopoldina (Postdoctoral fellowship LPDS2020-04 to M.T.) is gratefully acknowledged. We thank Dr. J. Taylor, Dr. A. A. Pogodaev and G. Bojanov (all Radboud University Nijmegen) for fruitful discussions and experimental advice.

Conflict of Interest

The authors declare no conflict of interest.

Keywords: enzymatic systems · enzymes · photochemistry · photoswitchable inhibitors · systems chemistry

[1] U. S. Bhalla, R. Iyengar, *Science* **1999**, *283*, 381–387.
[2] L. J. Sweetlove, A. R. Fernie, *Nat. Commun.* **2018**, *9*, 1–12.
[3] J. J. Tyson, B. Novák, *Annu. Rev. Phys. Chem.* **2010**, *61*, 219–240.
[4] R. Milo, S. Shen-Orr, S. Itzkovitz, N. Kashtan, D. Chklovskii, U. Alon, *Science* **2002**, *298*, 824–827.
[5] S. H. Strogatz, *Nature* **2001**, *410*, 268–276.
[6] A. Bashan, R. P. Bartsch, J. W. Kantelhardt, S. Havlin, P. C. Ivanov, *Nat. Commun.* **2012**, *3*, 1–9.
[7] R. F. Ludlow, S. Otto, *Chem. Soc. Rev.* **2008**, *37*, 101–108.
[8] G. Ashkenasy, T. M. Hermans, S. Otto, A. F. Taylor, *Chem. Soc. Rev.* **2017**, *46*, 2543–2554.
[9] B. A. Grzybowski, W. T. S. Huck, *Nat. Nanotechnol.* **2016**, *11*, 585–592.
[10] N. Singh, B. Lainer, G. J. M. Formon, S. De Piccoli, T. M. Hermans, *J. Am. Chem. Soc.* **2020**, *142*, 4083–4087.
[11] I. Maity, D. Dev, K. Basu, N. Wagner, G. Ashkenasy, *Angew. Chem. Int. Ed.* **2020**, *60*, 4512–4517.
[12] C. C. Robertson, T. Kosikova, D. Philp, *J. Am. Chem. Soc.* **2020**, *142*, 11139–11152.
[13] S. P. Afrose, S. Bal, A. Chatterjee, K. Das, D. Das, *Angew. Chem. Int. Ed.* **2019**, *58*, 15783–15787; *Angew. Chem.* **2019**, *131*, 15930–15934.
[14] B. A. K. Kriebisch, A. Jussupow, A. M. Bergmann, F. Kohler, H. Dietz, V. R. I. Kaila, J. Boekhoven, *J. Am. Chem. Soc.* **2020**, *142*, 20837–20844.
[15] D. E. Atkinson, *Annu. Rev. Biochem.* **1966**, *35*, 85–124.
[16] G. G. Hammes, C. W. Wu, *Science* **1971**, *172*, 1205–1211.
[17] C. M. Agapakis, P. M. Boyle, P. A. Silver, *Nat. Chem. Biol.* **2012**, *8*, 527–535.
[18] B. Alberts, *Cell* **1998**, *92*, 291–294.
[19] I. Willner, S. Rubin, *Angew. Chem. Int. Ed.* **1996**, *35*, 367–385; *Angew. Chem.* **1996**, *108*, 419–439.
[20] G. Mayer, A. Heckel, *Angew. Chem. Int. Ed.* **2006**, *45*, 4900–4921; *Angew. Chem.* **2006**, *118*, 5020–5042.
[21] C. Brieke, F. Rohrbach, A. Gottschalk, G. Mayer, A. Heckel, *Angew. Chem. Int. Ed.* **2012**, *51*, 8446–8476; *Angew. Chem.* **2012**, *124*, 8572–8604.
[22] J. Broichhagen, J. A. Frank, D. Trauner, *Acc. Chem. Res.* **2015**, *48*, 1947–1960.
[23] W. Szymański, J. M. Beierle, H. A. V. Kistemaker, W. A. Velema, B. L. Feringa, *Chem. Rev.* **2013**, *113*, 6114–6178.
[24] K. Hüll, J. Morstein, D. Trauner, *Chem. Rev.* **2018**, *118*, 10710–10747.
[25] C. Claaßen, T. Gerlach, D. Rother, *Adv. Synth. Catal.* **2019**, *361*, adsc.201900169.
[26] M. W. H. Hoorens, W. Szymanski, *Trends Biochem. Sci.* **2018**, *43*, 567–575.
[27] A. A. Pogodaev, A. S. Y. Wong, W. T. S. Huck, *J. Am. Chem. Soc.* **2017**, *139*, 15296–15299.
[28] J. Deng, D. Bezold, H. J. Jessen, A. Walther, *Angew. Chem. Int. Ed.* **2020**, *59*, 12084–12092; *Angew. Chem.* **2020**, *132*, 12182–12190.
[29] M. Teders, A. A. Pogodaev, G. Bojanov, W. T. S. Huck, *J. Am. Chem. Soc.* **2021**, *18*, jacs.0c12956.
[30] F. Markwardt, H. Landmann, P. Walsmann, *Eur. J. Biochem.* **1968**, *6*, 502–506.
[31] K. Tanizawa, S. Ishii, K. Hamaguchi, Y. Kanaoka, *J. Biochem.* **1971**, *69*, 893–899.
[32] M. T. Stubbs, *J. Med. Chem.* **1998**, *41*, 5445–5456.
[33] H. M. D. Bandara, S. C. Burdette, *Chem. Soc. Rev.* **2012**, *41*, 1809–1825.
[34] A. A. Pogodaev, C. L. Fernández Regueiro, M. Jakštaitė, M. J. Hollander, W. T. S. Huck, *Angew. Chem. Int. Ed.* **2019**, *58*, 14539–14543; *Angew. Chem.* **2019**, *131*, 14681–14685.
[35] S. Ludwanowski, O. Skarsetz, G. Creusen, D. Hoenders, P. Straub, A. Walther, *Angew. Chem. Int. Ed.* **2021**, *60*, 4358–4367; *Angew. Chem.* **2021**, *133*, 4404–4413.
[36] B. Helwig, B. van Sluijs, A. A. Pogodaev, S. G. J. Postma, W. T. S. Huck, *Angew. Chem. Int. Ed.* **2018**, *57*, 14065–14069; *Angew. Chem.* **2018**, *130*, 14261–14265.
[37] M. J. Hansen, W. A. Velema, M. M. Lerch, W. Szymanski, B. L. Feringa, *Chem. Soc. Rev.* **2015**, *44*, 3358–3377.
[38] M. M. Lerch, M. J. Hansen, W. A. Velema, W. Szymanski, B. L. Feringa, *Nat. Commun.* **2016**, *7*, 1–10.
[39] A. S. Lubbe, W. Szymanski, B. L. Feringa, *Chem. Soc. Rev.* **2017**, *46*, 1052–1079.
[40] M. W. Haydell, M. Centola, V. Adam, J. Valero, M. Famulok, *J. Am. Chem. Soc.* **2018**, *140*, 16868–16872.
[41] R. J. Mart, R. K. Allemann, *Chem. Commun.* **2016**, *52*, 12262–12277.
[42] J. N. Weiss, *FASEB J.* **1997**, *11*, 835–841.

Manuscript received: April 28, 2021
Version of record online: ■■, ■■■

ARTICLES

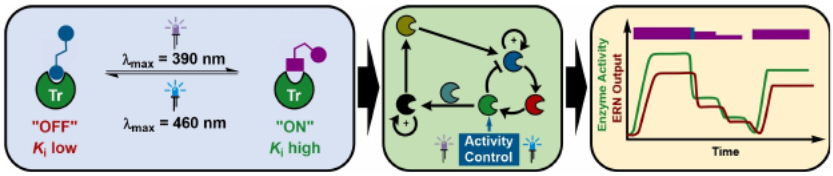

*Dr. M. Teders, N. R. Murray, Prof. W. T. S. Huck**

Let there be light! A regulatory strategy enabling to fine-tune the kinetics of enzyme-catalyzed reactions under out-of-equilibrium conditions is exploited. By synthesis and incorporation of reversible photoswitchable inhibitors, the output of bottom-up constructed enzymatic systems could be controlled using light. In addition, two enzymes were independently photoregulated in a bi-enzymatic system using light of different wavelengths.